Growth of thin films of molybdenum and tungsten oxides by combustion CVD using aqueous precursor solutions

Davis, MJ, Benito, G, Sheel, DW and Pemble, ME

http://dx.doi.org/10.1002/cvde.200306260

Growth of Thin Films of Molybdenum and Tungsten Oxides by Combustion Chemical Vapour Deposition using Aqueous Precursor Solutions.

Martin J. Davis*, Guillermo Benito, David W. Sheel, Martyn E. Pemble.

Institute of Materials Research, University of Salford, Salford, M5 4WT, UK

Fax: 0161 295 5272, E-mail: m.j.davis@salford.ac.uk

Using combustion chemical vapour deposition, layers of molybdenum and tungsten oxides have been deposited on glass and silicon at low temperatures. Inexpensive ammonium salts of molybdate and metatungstate ions were used as precursors and were delivered to the coating flame as an aqueous solution using a nebuliser. The resulting films were analysed by scanning electron microscopy (SEM), energy dispersive analysis of X-rays (EDAX), Rutherford backscattering (RBS), X-ray photoelectron spectroscopy (XPS) and X-ray diffraction (XRD). These indicate that the films are continuous, moderately smooth and consist of amorphous, disordered molybdenum and tungsten trioxides.

1. Introduction

Molybdenum and tungsten oxide thin films have a number of applications including use in coating structures to produce electrochromic displays and “smart” glass and as components of gas sensors.[1-3] Coatings have been produced by a wide variety of techniques including sol-gel,[4-6] spin-coating,[7] electrochemical deposition,[8] vacuum physical vapour deposition (PVD),[9-13] thermal chemical vapour deposition (CVD)[14, 15] and spray pyrolysis.[16-18] Solution methods are widely used but can result in film structural and durability constraints.

Vacuum PVD methods produce good quality films, but have very high capital cost for high-throughput coating of large samples, and are complex to integrate for continuous processes.

Combustion chemical vapour deposition is a relatively new technique for the general growth of thin films.[19, 20] Precursors are dissolved in a flammable solvent and the solution delivered to a burner where it is ignited to give a flame. The substrate is then passed repeatedly under the flame to build up a coating.[21-23] One advantage of this technique is that deposition can be performed at low substrate temperatures, since the energy for decomposition of the precursor is provided by the flame. In addition, because the flame temperature is very high, thermally unstable precursors are not necessarily required. Deposition of molybdenum and tungsten oxides by this technique has been reported previously,[24] but no details of reaction conditions or film properties were given.

In this paper we present the deposition and analysis of molybdenum oxide and tungsten oxide films using combustion CVD. In contrast to the earlier technique cited above, our system uses a self-supporting propane-oxygen-nitrogen flame into which the precursor is introduced. This is achieved by mixing the precursor, in this case as a nebulised solution, into the combustion gas stream just before the burner head. Therefore the solvent does not need to be flammable and we have used water since it is cheap, readily handled and environmentally benign.

2. Results and Discussion

The principle aim in this project was to demonstrate that clear, even, continuous films of molybdenum and tungsten oxides with at least sufficient hardness and adhesion to be readily handled could be rapidly deposit using combustion CVD. In order to do this it was necessary to determine growth parameters which would, as much as possible, maximise these general

properties. The aim at this stage was not to fully optimise conditions for production of films exceeding specific, predefined, quantitative properties. An initial set of experiments was performed in which various growth parameters were varied individually and the results on the produced films determined qualitatively by visual inspection and wiping the surface. Interference fringes were used as a guide to relative film thickness. The results are shown in Table 1. The process of determining a set of conditions giving films with the desired properties was based on this experience. It consisted of making changes to individual deposition parameters and accepting those which gave better films according to the selected criteria (good clarity, visible continuity, evenness, hardness and adhesion of the films, minimal loose powder and high growth rate), and rejecting those which produced worse films. Repeat coatings were also made to assess qualitative reproducibility and parameter changes which led to poorer reproducibility were also rejected. Increasingly small parameter changes were used until no change in the coating or reproducibility of growth could be observed. The set of conditions obtained represent the selected conditions for growth.

Two additional parameters which may be important but which could not be directly adjusted in our process are aerosol droplet size and flame temperature. These are both difficult to measure reliably and such measurements are outside the scope of this work. However, the specification for the nebuliser used gives a droplet size range of 1 to 5 μm with an average of about 3 μm. Possibly because of this small droplet size, deposition of precursor inside the burner head was found to be minimal and blocking was not a problem. Published adiabatic flame temperatures for near-stoichiometric propane air flames are about 2250 K with a drop of at most a few hundred Kelvin expected on increasing the equivalence ratio to 1.6.[25] Introduction of the nebulised solution into the flame would be expected to effect the temperature. However, the power absorbed by the evaporation and heating of water introduced into the flame can be calculated using published values of the variation of the

enthalpy of water with temperature.[26] At the maximum rate used here (0.22 $cm^3.min^{-1}$) this is only 26 W, less than 2% of the total flame power of 1.5 kW, so the cooling is not likely to be very significant.

Using the selected conditions, a number of films were grown for analysis. Aspects of the microscopic physical structure of the coatings such as thickness, surface roughness and continuity, were examined by SEM. Chemical analysis by EDAX was used to ascertain that the films were indeed the metal oxides and RBS gave their stoichiometry. XRD and XPS were used to obtain further information on the films such as their crystallinity and the chemical environments and oxidation states of the metal atoms.

A coating grown on glass using 30 passes, ammonium molybdate as precursor and with the selected conditions was light grey in colour, free of visible powder and adherent, resisting vigorous rubbing. An SEM image of the above film on glass is shown in Fig. 1 together with the EDAX analysis. The SEM shows a fractured edge of the film and substrate. The fracturing was performed in a manner which shows clearly the films on the glass. It gives a clean vertical break in the film or films on the glass, but a break in the glass substrate which slopes away from the fractured film edge. From the SEM image the film thickness can be estimated at 30 nm. The film appears to be continuous but, while the underlying film is moderately smooth, has a number of surface features ranging in size from about 50 to 1000 nm across where the film appears to be considerably thicker. The EDAX analysis confirms the presence of molybdenum in the film. Since the penetration depth of EDAX (*ca*. 1 μm) is much greater than the film thickness, components from the underlying substrate also appear. These are silicon, oxygen, sodium and calcium, together with smaller amounts of magnesium and aluminium, all of which are normally present in soda-lime glass.

Using the chosen conditions for the ammonium metatungstate precursor, a film grown on silica-coated glass with 30 passes was similarly adherent and free of powder but was a pale yellow-brown in colour. Fig. 2 shows an SEM of the fractured edge of the film and substrate, together with EDAX analysis. The silica coating can be seen as a layer about 30 nm thick on the glass with the CCVD deposited film of about 20 nm thickness on top of this. The film is continuous with a number of surface structures varying between about 20 and 100 nm in size, though the underlying film appears moderately smooth. The EDAX analysis shows the presence of tungsten in the film but also a little molybdenum. This molybdenum arose due to ineffective cleaning of the nebuliser from a previous run with molybdenum precursor. The cleaning protocol was henceforth improved to eliminate this. Other peaks in the EDAX are from the substrate as explained above.

In order to ascertain that the films were metal oxides and to determine their stoichiometries, films were grown under the same conditions to those above, but on silicon wafers. These films were then analysed by RBS. The results for the molybdenum containing film (Fig. 3) shows that it is indeed molybdenum oxide, with no other elements apart from the silicon of the substrate and its thin coating of silicon oxide evident. The stoichiometry is MoO_3 and the film is estimated to be 33 nm thick. Similarly, for the tungsten containing film (Fig. 4), it is shown to be only tungsten oxide with an overall stoichiometry of WO_3. However, the tungsten peak shows considerable asymmetry, with significant intensity at lower energies, and thus greater apparent depth, than would be expected for a simple film of uniform thickness. This is probably because the film is of variable thickness and the simulation shown uses a model with different percentages of coverage for parts of the film with different discreet thickness. In reality the film would probably have continuously variable thickness due to surface roughness. This is supported by the SEM of the film grown

under the same conditions on glass (Fig. 2) which show considerable roughness and surface features. From this model the average film thickness is 32 nm.

Although RBS gives reliable measurement of overall stoichiometry, it gives no information on the chemical nature of the phase or phases present. Therefore thicker films on silicon, grown by increasing the number of passes under the flame to 300, were analysed by XRD and XPS. For both the molybdenum and tungsten oxide films, the XRD gave an essentially unstructured background with, at best, a few extremely small and broad peaks which could not be fit to known materials with any confidence. It would therefore appear that the films are essentially amorphous.

XPS spectra of both the surface and the interior of the film as exposed by ion etching are shown for the molybdenum oxide film in Fig. 5. The two main peaks for the surface correspond well to the $3d_{5/2}$, $3d_{3/2}$ doublet[27] of MO_3, but the peaks are very broad. This suggests that the molybdenum atoms are in a range of different coordination environments and therefore that the film is amorphous and the structure somewhat disordered. This is consistent with the XRD results. In addition there is a small shoulder on the low energy side of the main peak, at about 230 eV. This may indicate a reduced form of the metal and a slight departure from true MoO_3 stoichiometry.[28] The spectrum of the interior of the film would seem to suggest that it consists of MO_2, though again the peaks are rather broad. However, this may be due to reduction of the film by preferential sputtering of oxygen by the ion etch beam, a well-known effect on molybdenum and tungsten oxides.[29] This interpretation is supported by the RBS results, which would have shown a much lower O:Mo ratio if significant MO_2 was present in the films as grown.

The XPS spectra of the tungsten oxide film (Fig. 6) show a rather similar situation. The surface spectrum shows the $4f_{7/2}$, $4f_{5/2}$ doublet[30] of WO_3 with the broadness of the peaks

indicating significant variation in the coordination environments around the tungsten atoms. However, no additional peaks can be observed. The spectrum of the film interior clearly shows the tungsten metal $4f_{7/2}$ peak on the low energy side, but the $4f_{5/2}$ peak is larger than would be expected. This is probably due to the presence of WO_2, the $4f_{7/2}$ peak of which will largely overlap the metal $4f_{5/2}$ peak. There also appears to be some remaining WO_3. Again, the presence of these reduced forms is likely to be due to reduction by the ion etching beam.

3. Conclusions

It has been shown that combustion CVD can be used to deposit thin films of molybdenum and tungsten oxides from aqueous solutions of cheap, readily available precursors. The growth at low substrate temperatures gave amorphous films of pure oxide with stoichiometries close to those of the trioxides. Careful selection of the growth parameters allowed the growth of continuous films, which adhere well to the substrates and, despite quite a few surface irregularities, show a moderately smooth underlying surface. It is suggested that the combustion CVD route described here might be suitable for the production of a range of molybdenum and tungsten oxide coatings in a variety of industrial coating environments.

4. Experimental

4.1. C-CVD System

A schematic of the combustion CVD system is shown in Fig. 7. The burner head was specifically conceived to give a uniform flame suitable for coating over a moderately large area. It has four rows of small holes in the burner plate giving an overall flame about 100 mm long and 10 mm wide, consisting of many individual flame cones with a total aperture area of 260 mm^2. This is fed with a mixture of propane, oxygen and nitrogen to produce the flame

(Fig. 8). Precursors are delivered in a nitrogen gas stream either as a vapour from a bubbler or as an aerosol from a nebuliser and are introduced into the combustion gas mixture just before the burner head. The nebuliser used was a commercial ultrasonic unit (Sunrise Medical). All gas flows are controlled using digital mass flow controllers operated from a PC. Custom software automatically calculates and adjusts the gas flows based on flame parameters. These are the power, calculated from the combustion enthalpy of the propane, the equivalence ratio, defined as the ratio of the flow of propane to that of oxygen, taking account of the 1 to 5 stoichiometry of combustion, (i.e. the equivalence ratio equals five times the propane flow divided by the oxygen flow) and oxygen percentage in the oxygen-nitrogen mix. The system also compensates for the nitrogen flow through the precursor delivery system. Non-return valves and filters in the fuel and oxidiser lines protect against possible flashback. These lines also contain solenoid valves linked to a flame detector in order to automatically isolate the flows in a flame-out condition.

The substrate is supported on a stainless steel plate, the same width as the length of the burner head, on a graphite susceptor on which it can be heated if required. This stage is height adjustable to allow the burner head-substrate distance to be varied. The susceptor is mounted on a motor-driven reciprocating translation stage allowing the substrate to be passed back and forth under the flame (Fig. 8). The speed and number of passes are controlled automatically.

4.2. Deposition conditions

All the films reported in this paper were deposited using nebulisation precursor delivery. A wide range of conditions for precursor deliver, combustion, and deposition were tried. However, the chosen conditions were as follows. Molybdenum oxide was deposited using a 0.1 M solution of ammonium molybdate $\{(NH_4)_6Mo_7O_{24}\}$ and tungsten oxide from a 0.05 M solution of ammonium metatungstate $\{(NH_4)_6H_2W_{12}O_{40}\}$, the solvent in both cases being

deionised water. The burner head – substrate distance was 3 to 4 mm and the susceptor was heated to 100 ºC to prevent any possibility of water condensation. Between 30 to 300 passes at 50 mm.s^{-1} were used, depending on the thickness of film required. The burner head was supplied with 1 SLM of propane, 3.7 SLM of oxygen and 13.9 SLM of nitrogen corresponding to a power of 1.5 kW, equivalence ratio of 1.35 and an oxygen concentration of 21%. For molybdenum oxide deposition, 0.75 SLM of the total nitrogen flow was used to carry the nebulised precursor solution giving a delivery rate of 0.097 cm^3.min^{-1}, whereas for tungsten oxide this was 0.85 SLM (0.11 cm^3.min^{-1}). Films were deposited on substrates of silicon wafer (35 x 20 x 0.5 mm), glass microscope slides (76 x 26 x 1 mm) or silica coated float-glass (76 x 26 x 3 mm), placed with their long axes across the width of the substrate holder. Immediately before coating, substrates were cleaned with water and detergent, rinsed thoroughly with water and de-ionised water and allowed to dry.

4.3. Analysis instrumentation

SEM images were obtained using a Philips XL30 with Phoenix EDAX spectrometer. All SEM images shown here were recorded using a beam energy of 30 kV and a magnification of times 50K. XPS were recorded on Kratos Axis 165 or Amicus spectrometers while XRD data was recorded on a Philips PW1130 diffractometer. RBS measurements were made using a 2 MeV accelerator and He^+ analysing beam at normal incidence and scattering angle of 168º in IBM geometry. The RBS data were compared with simulation data from a model using the Quark software package.

Acknowledgements

We would like to thank the following. CEC for funding under 5th Framework Growth Programme (G5RD-CT 1999-00160) and IHF funding for GB. Dr. R. Weidl and Mr. T.

Richter of Innovent e.V., Jena, for advice on setting up the CCVD system. The Science Support Group at Pilkington Technology Management Limited for SEM, EDAX, XPS and XRD analysis. Dr. R. Valizadeh of Manchester Metropolitan University for RBS carried out at Salford University.

References

[1] C. G. Granqvist, *Sol. Energy Mater. Sol. Cells* **2000**, 60, 201.

[2] N. Miyata, S. Akiyoshi, *J. Appl. Phys.* **1985**, 58, 1651.

[3] S. C. Moulzolf, S. A. Ding, R. J. Lad, *Sens. Actuator B-Chem.* **2001**, 77, 375.

[4] K. D. Lee, *Thin Solid Films* **1997**, 302, 84.

[5] J. P. Cronin, D. J. Tarico, J. C. L. Tonazzi, A. Agrawal, S. R. Kennedy, *Sol. Energy Mater. Sol. Cells* **1993**, 29, 371.

[6] J. Wang, J. M. Bell, I. L. Skryabin, *Sol. Energy Mater. Sol. Cells* **1999**, 56, 465.

[7] K. Hinokuma, A. Kishimoto, T. Kudo, *J. Electrochem. Soc.* **1994**, 141, 876.

[8] A. Guerfi, L. H. Dao, *J. Electrochem. Soc.* **1989**, 136, 2435.

[9] R. J. Colten, A. M. Guzman, J. W. Rabalais, *J. Appl. Phys.* **1978**, 49, 409.

[10] C. Cantalini, M. Pelino, H. T. Sun, M. Faccio, S. Santucci, L. Lozzi, M. Passacantando, *Sens. Actuator B-Chem.* **1996**, 35, 112.

[11] M. Penza, M. A. Tagliente, L. Mirenghi, C. Gerardi, C. Martucci, G. Cassano, *Sens. Actuator B-Chem.* **1998**, 50, 9.

[12] N. Yoshiike, Y. Mizuno, S. Kondo, *J. Electrochem. Soc.* **1984**, 131, 2634.

[13] M. S. Burdis, J. R. Siddle, *Thin Solid Films* **1994**, 237, 320.

[14] E. P. S. Barrett, G. C. Georgiades, P. A. Sermon, *Sens. Actuator B-Chem.* **1990**, 1, 116.

[15] P. V. Ashrit, *Thin Solid Films* **2001**, 385, 81.

[16] P. S. Patil, P. R. Patil, E. A. Ennaoui, *Thin Solid Films* **2000**, 370, 38.

[17] D. Craigen, A. Mackintosh, J. Hickman, K. Colbow, *J. Electrochem. Soc.* **1986**, 133, 1529.

[18] M. Regragui, M. Addou, A. Outzourhit, J. C. Bernede, E. E. Idrissi, E. Benseddik, A. Kachouane, *Thin Solid Films* **2000**, 358, 40.

[19] A. T. Hunt, W. B. Carter, J. K. Cochran, *Appl. Phys. Lett.* **1993**, 63, 266.

[20] A. T. Hunt, J. K. Cochran, W. B. Carter, *US Patent 5 652 021*, **1997**.

[21] T. A. Polley, W. B. Carter, *Thin Solid Films* **2001**, 384, 177.

[22] J. McHale, R. W. Schaeffer, A. Kebede, J. Macho, R. E. Salomon, *J. Supercond.* **1992**, 5, 511.

[23] M. R. Hendrick, H. Shao, T. J. Hwang, A. T. Hunt, *Surf. Modif. Technol.* **1998**, 12, 163.

[24] J. J. Schmitt, *Symposium on Properties and Processing of Vapor-Deposited Coatings*, **1999**, 555, 255.

[25] R. M. Fristrom, *Flame structure and processes*, Oxford University Press, New York **1995**.

[26] I. Barin, *Thermochemical Data of Pure Substances*, VCH, Weinheim **1993**.

[27] S. I. Castaneda, I. Montero, J. M. Ripalda, N. Diaz, L. Galan, F. Rueda, *J. Appl. Phys.* **1999**, 85, 8415.

[28] P. A. Spevack, N. S. McIntyre, *J. Phys. Chem.* **1993**, 97, 11020.

[29] T. J. Driscoll, L. D. McCormick, W. C. Lederer, *Surf. Sci.* **1987**, 187, 539.

[30] G. Leftheriotis, S. Papaefthimiou, P. Yianoulis, A. Siokou, *Thin Solid Films* **2001**, 384, 298.

Table 1. Qualitative effect on deposited films of variation in individual growth condition parameters.

Parameter	Range	Qualitative effect on film over parameter range	
		MoO_x	WO_x
Solution concentration ($mol.dm^{-3}$)	molybdate: 0.05-0.25 tungstate: 0.03-0.15	increasing thickness grey to brown no powder to moderate powder decreasing hardness/adhesion	increasing thickness yellow to brown no powder to all powder decreasing hardness/adhesion
Solution delivery rate ($cm^3.min^{-1}$)	0.06-0.22	increasing thickness grey to brown no powder to slight powder	increasing thickness yellow to brown no powder to much powder
Head-substrate distance (mm)	3-30	decreasing thickness no powder to slight powder	decreasing thickness no powder to much powder
Susceptor temperature (°C)	20-300	decreasing thickness	decreasing thickness
Equivalence ratio	1.0-1.6	grey to brown	blue to green to brown to grey no powder to slight powder

Figure Captions

Figure 1. SEM and EDAX of a molybdenum oxide thin film on a glass (microscope slide) substrate. The SEM is of the fractured edge of the sample viewed at a tilt angle of 80º, allowing both the surface and cross section of the film to be observed.

Figure 2. SEM and EDAX of a tungsten oxide thin film on a silica coated float-glass substrate. The SEM is of the fractured edge of the sample viewed at a tilt angle of 80º, allowing both the surface and cross section of the film to be observed.

Figure 3. RBS spectrum for a molybdenum oxide thin film on a silicon substrate.

Figure 4. RBS spectrum for a tungsten oxide thin film on a silicon substrate.

Figure 5. XPS of molybdenum 3d core levels for a molybdenum oxide thin film.

Figure 6. XPS of tungsten 4f core levels for a tungsten oxide thin film.

Figure 7. Schematic of the combustion CVD deposition system.

Figure 8. Photograph of the burner head and the flame during coating of a float-glass substrate (microscope slide).

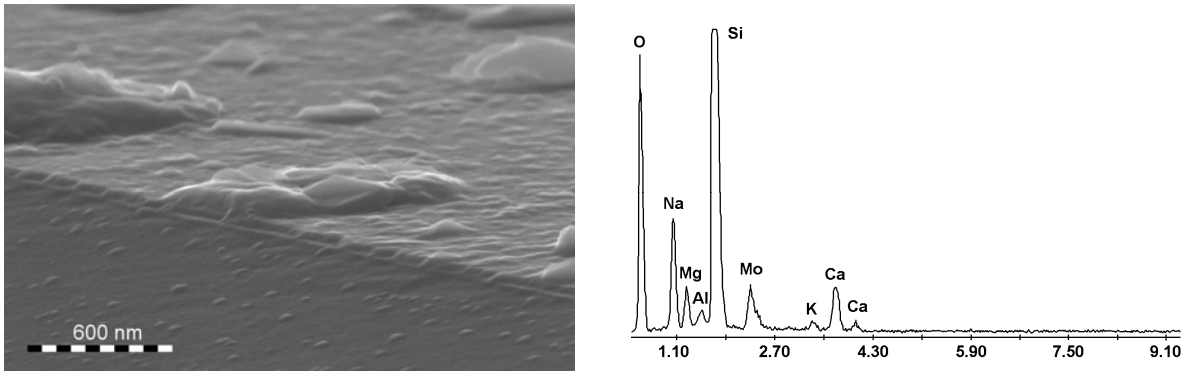

M. J. Davis, Figure 1.

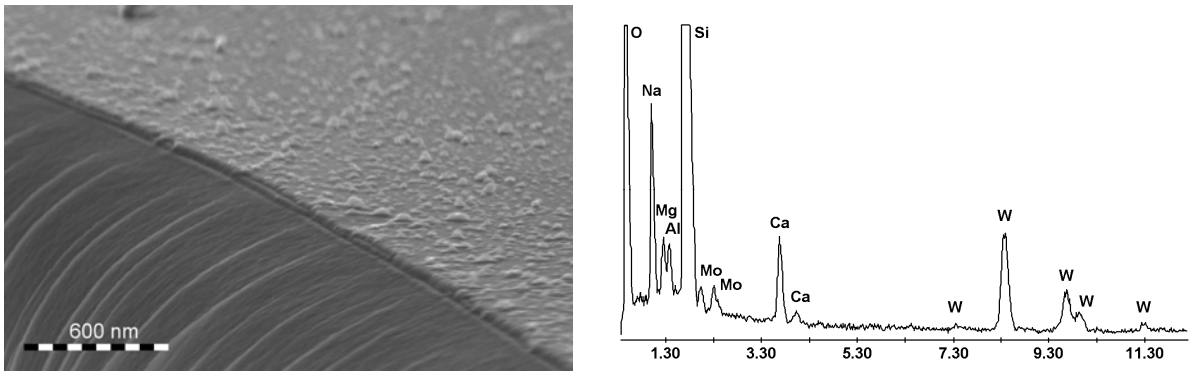

M. J. Davis, Figure 2.

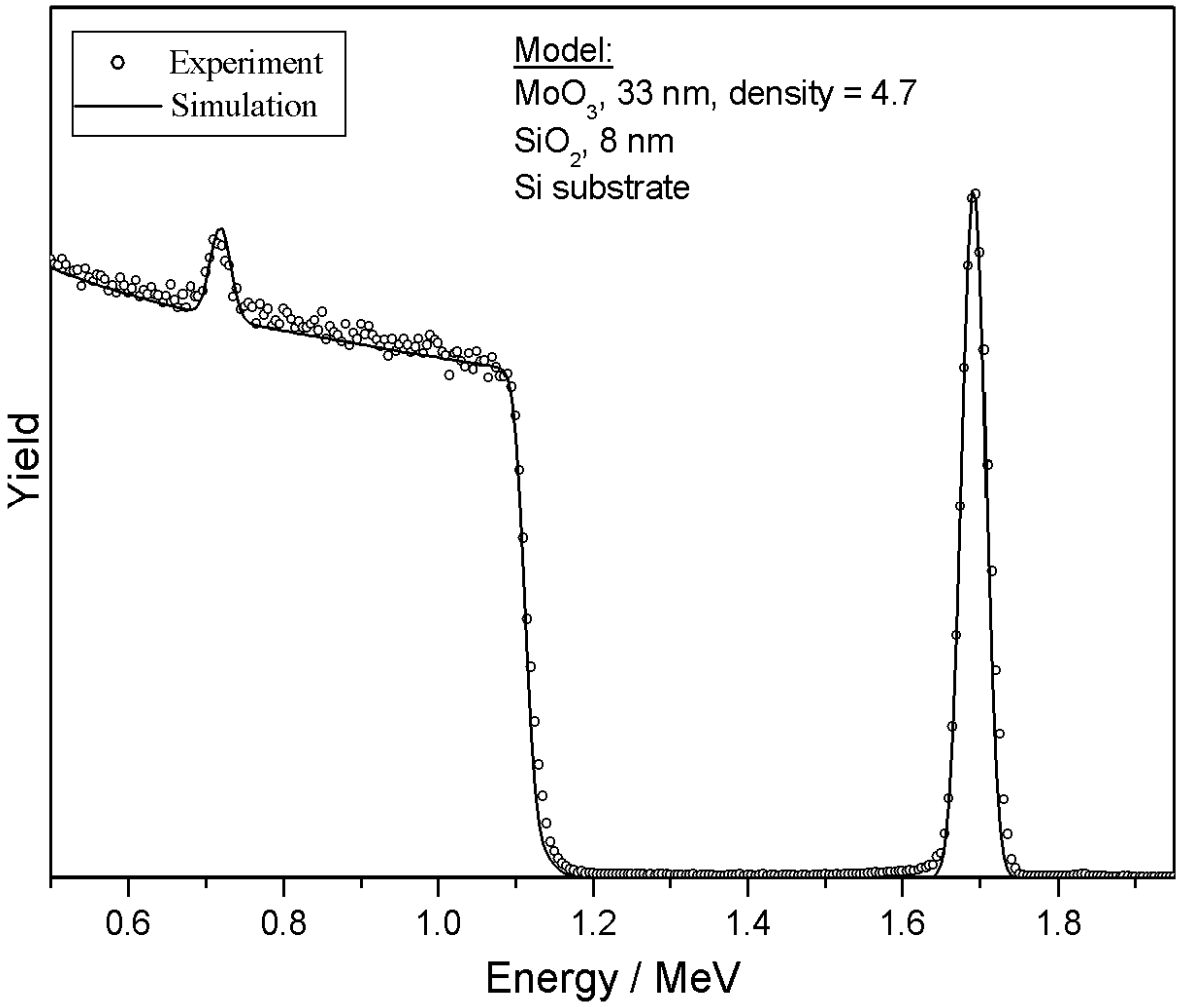

M. J. Davis, Figure 3.

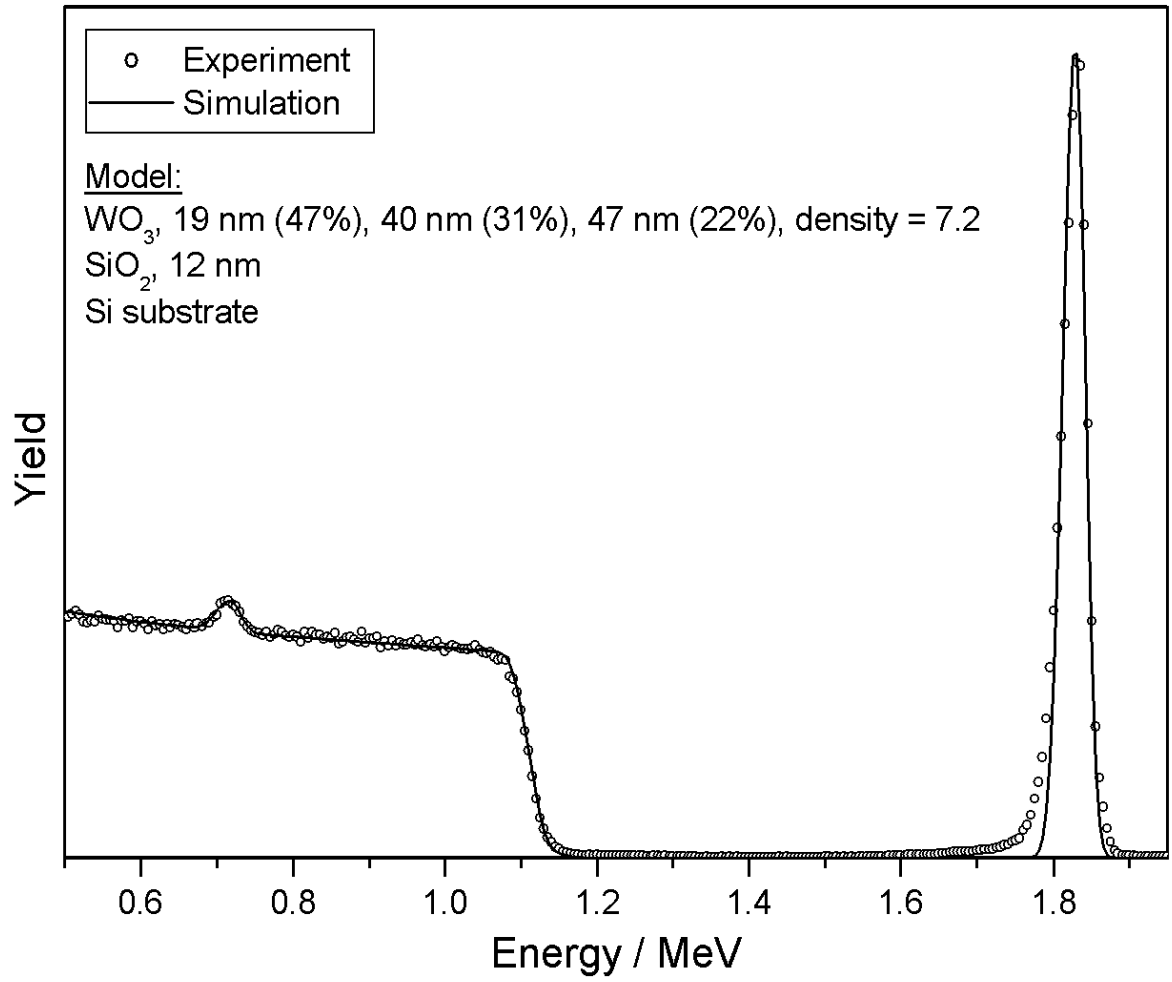

M. J. Davis, Figure 4.

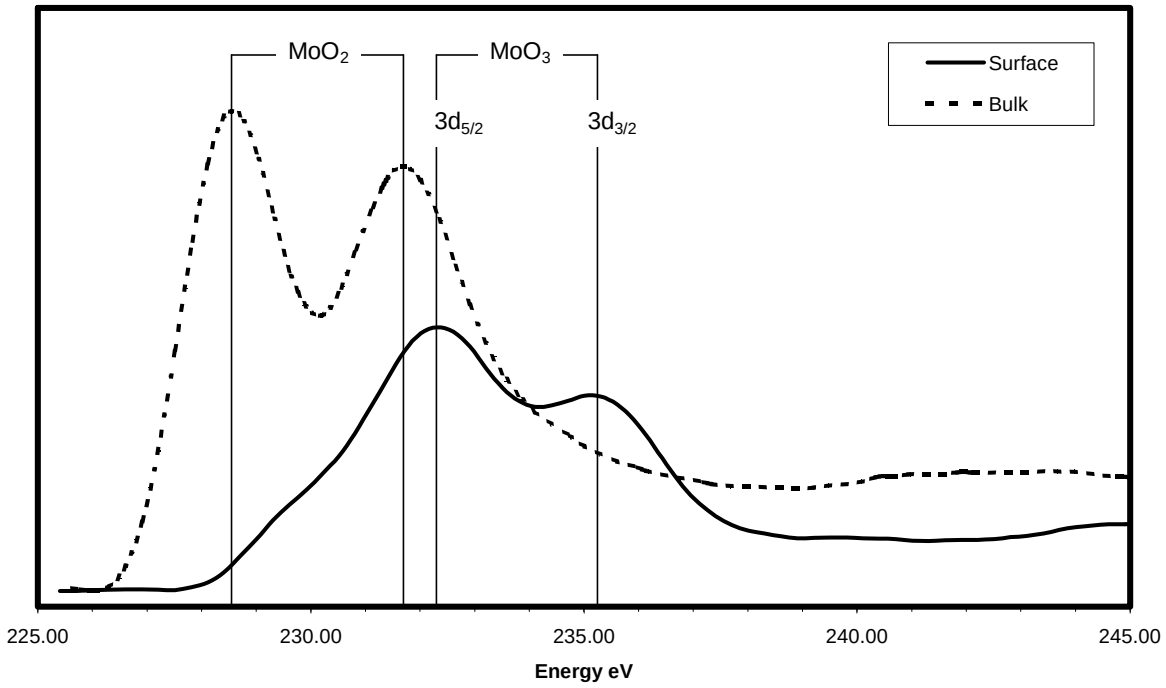

M. J. Davis, Figure 5.

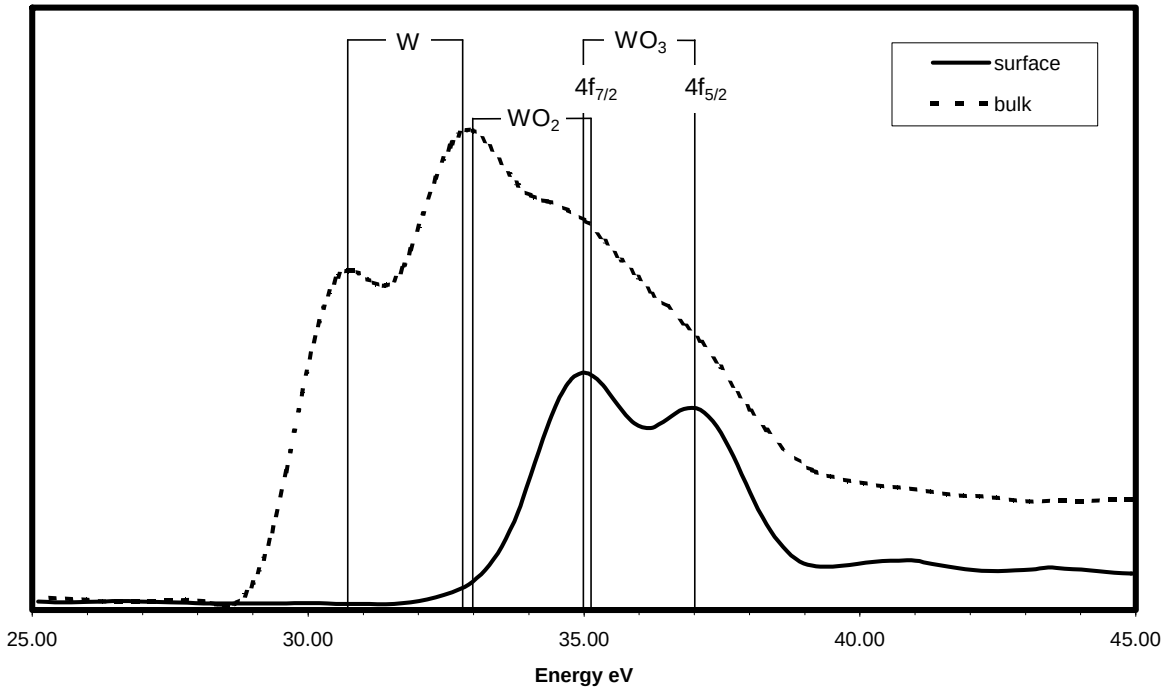

M. J. Davis, Figure 6.

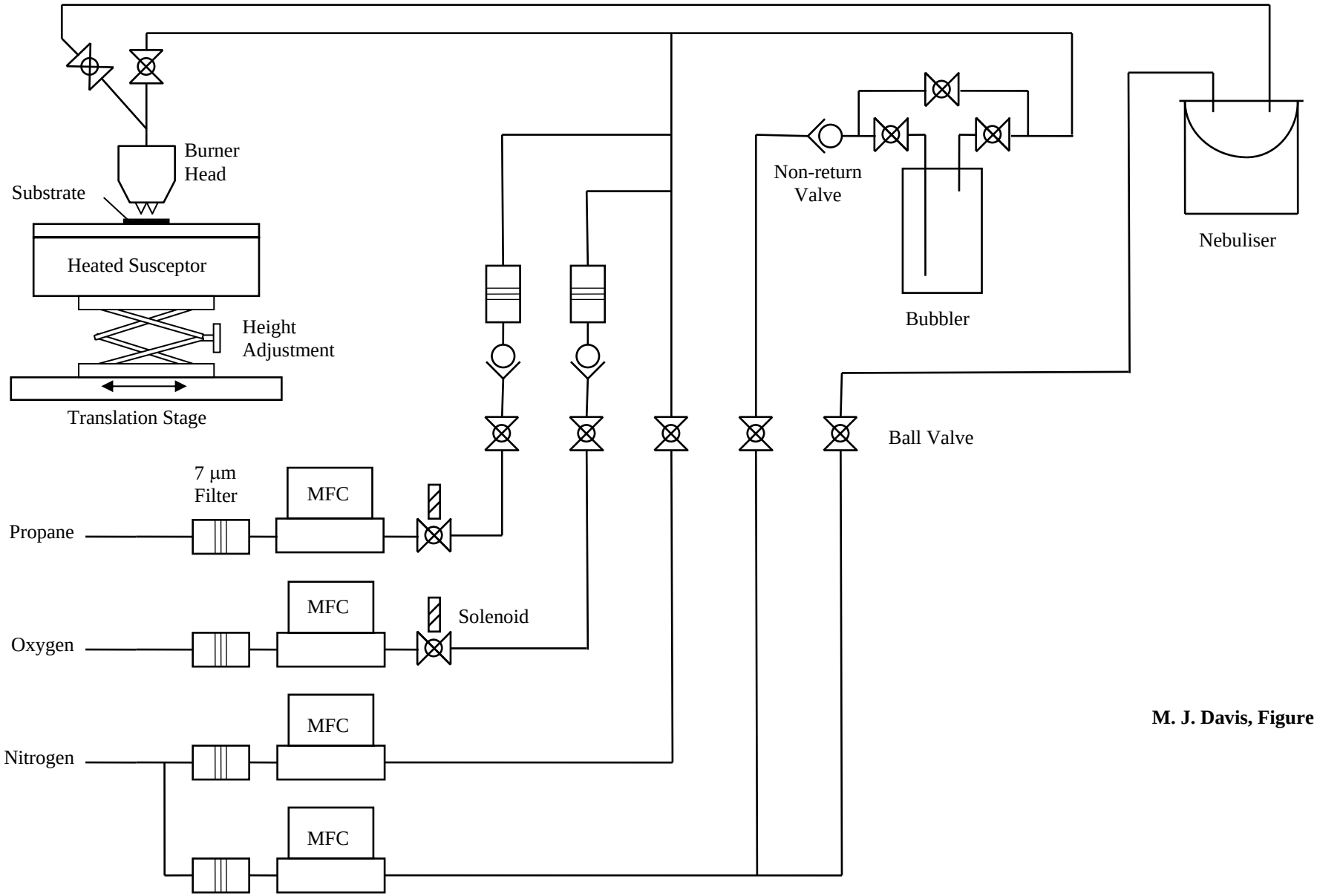

M. J. Davis, Figure 7.

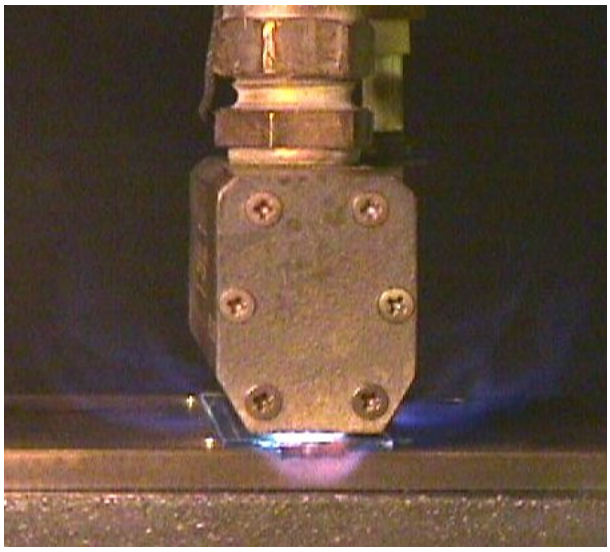

M. J. Davis, Figure 8.